Organometallics **2007,** *26,* 56−64

DFT Study of Hydride Exchange in a Binuclear Ruthenium Complex

Samat Tussupbayev and Sergei F. Vyboishchikov*

Institut de Química Computacional, Campus de Montilivi, Universitat de Girona, 17071 Girona, Catalonia, Spain

Received August 2, 2006

This paper presents a DFT study of hydrogen exchange in the binuclear polyhydride complex CpRu(μ-H)$_4$RuCp (**1**) with molecular hydrogen. Both dissociative (through the CpRu(μ-H)$_2$RuCp intermediate) and associative mechanisms (through hydrogen coordination to yield intermediates Cp$_2$Ru$_2$H$_6$ and subsequent hydrogen dissociation) are considered. The calculations show that the dissociative pathway has a prohibitively high barrier for hydrogen dissociation, with $\Delta G^{\ddagger}_{298}$ about 34 kcal·mol^{-1}. The associative mechanism is much more favorable. There are, in turn, two possible pathways, going through either *cis*-Cp(H)$_2$Ru(μ-H)$_2$Ru(H)$_2$Cp (**2a**) or *trans*-Cp(H)$_2$Ru(μ-H)$_2$Ru(H)$_2$Cp (**2b**). The *cis* pathway is more favorable, with $\Delta G^{\ddagger}_{298}$ barriers for the rate-determining step of 24 kcal·mol^{-1}. The intermediate **2a** can either dissociate directly or undergo isomerization processes involving interchanging of bridging and terminal hydrides. Overall, the calculations support the associative pathway for the hydrogen exchange, but show that the details of the mechanism are rather complicated.

Introduction

Polynuclear transition metal complexes often exhibit unusual reactivity not found with mononuclear complexes.[1] In particular, the ruthenium polyhydride complexes exhibit diverse reactivity toward a variety of substrates. A substantial experimental work in this area has been performed by H. Suzuki and co-workers.[2a−f] A very versatile chemistry of such processes includes C−H bond activation, C−C coupling, olefin insertion into a C−C bond,[3] Si−H bond activation,[4] and a number of other insertion reactions of the binuclear complex Cp*Ru(μ-H)$_4$RuCp* (Cp* = pentamethylcyclopentadienyl).[5,6] On the other hand, the trinuclear complex (Cp*Ru)$_3$(μ-H)$_3$(μ_3-H)$_2$ effects, for instance, alkane activation,[7] C=C bond cleavage in olefins,[8] and N−N bond cleavage in hydrazine.[9]

A very characteristic feature of these complexes is a very high mobility of the hydride ligands, which manifests itself in an easy conversion between the bridging and terminal hydrides. The simplest example is given by the protonation reaction (Cp*Ru)$_3$(μ-H)$_3$(μ_3-H)$_2$ + H$^+$ → (Cp*Ru)$_3$(μ-H)$_6^+$.[10] This mobility greatly influences the ability of the complexes to coordinate an incoming ligand. Another process governing the chemistry of such complexes is the bridging ligand coordination to more than one metal center, with the manner of coordination changing during the course of the reaction. To mention just one example, the bis-vinyl complex Cp*(η^2-C$_2$H$_4$)Ru(CH=CH$_2$)$_2$-RuCp* contains C−Ru σ-bonds to one ruthenium atom while coordinating in the η^2-π-manner to the other.[3] Eventually, these two factors determine the cooperativity of multiple metal centers, which in turn controls the distinctive chemistry of the polyatomic polyhydride complexes.

The reaction of (Cp*Ru)$_3$(μ-H)$_3$(μ_3-H)$_2$ with cyclopentadiene leading to a C−C bond cleavage has attracted substantial attention[11] and was studied computationally by Khoroshun et al.[12] Contrary to Suzuki et al.'s original hypothesis, it was found that the reaction proceeds through an associative mechanism with a large number of intermediates. In this mechanism, many processes known in organometallic chemistry, such as oxidative addition, hydride−dihydrogen ligand isomerism, and agostic interactions, play an important role. It is obvious that, for reactions of such complexity, experimental studies alone, however comprehensive they may be, cannot reveal all the mechanistic details. Therefore, computational studies are an important complement to the experiment. Other computational studies regarding the reactivity of triruthenium complexes were published by Riehl et al.[13] and by Inagaki et al.[14]

Our computational research focuses on the chemistry of binuclear complex Cp*Ru(μ-H)$_4$RuCp* (**A**). In the present work, we investigate the simplest example of its reactivity, the hydride exchange process. The hydride ligands in **A** undergo intermolecular hydride exchange with dihydrogen under atmospheric

---

* Corresponding author. Fax: +34 972 418356. Tel: +34 972 418362. E-mail: vybo@stark.udg.es.

[1] (a) Adams, R. A.; Cotton, F. A. *Catalysis by Di- and Polynuclear Metal Cluster Complexes*; Wiley-VCH: New York, 1998. (b) Doherty, S. *Organometallic Chemistry of Bi- and Poly-nuclear Complexes*; Royal Society of Chemistry−Annual Reports−Book A, 1996; pp 395−432

[2] (a) Suzuki, H. *Eur. J. Inorg. Chem.* **2002**, 1009. (b) Takao, T.; Amako, M.; Suzuki, H. *Organometallics* **2003**, *22,* 3855. (c) Nakajima, Y.; Suzuki, H. *Organometallics* **2003**, *22,* 959. (d) Suzuki, H.; Kakigano, T.; Tada, K.; Igarashi, M.; Matsubara, K.; Inagaki, A.; Oshima, M.; Takao, T. *Bull. Chem. Soc. Jpn.* **2005**, *78*, 67. (e) Nakajima, Y.; Suzuki, H. *Organometallics* **2005**, *24,* 1860. (f) Shima, T.; Suzuki, H. *Organometallics* **2005**, *24,* 1703.

[3] Suzuki, H.; Omori, H.; Lee, D. H.; Yoshida, Y.; Fukushima, M.; Tanaka, M.; Moro-oka, Y. *Organometallics* **1994**, *13*, 1129.

[4] Takao, T.; Suzuki, H.; Tanaka, M. *Organometallics* **1994**, *13*, 2554.

[5] Tada, K.; Oishi, M.; Suzuki, H. *Organometallics* **1996**, *15*, 2422.

[6] Takao, T.; Yoshida, S.; Suzuki, H. *Organometallics* **2005**, *24*, 521.

[7] Inagaki, A.; Takemori, T.; Tanaka, M.; Suzuki, H. *Angew. Chem., Int. Ed.* **2000**, *39*, 404.

[8] Takemori, T.; Inagaki, A.; Suzuki, H. *J. Am. Chem. Soc.* **2001**, *123*, 1762.

[9] Nakajima, Y.; Suzuki, H. *Organometallics* **2003**, *22*, 959.

[10] Suzuki, H.; Kakigano, T.; Tada, K.; Igarashi, M.; Matsubara, K.; Inagaki, A.; Oshima, M.; Takao, T. *Bull. Chem. Soc. Jpn.* **2005**, *78*, 67.

[11] Suzuki, H.; Takaya, Y.; Takemori, T.; Tanaka, M. *J. Am. Chem. Soc.* **1994**, *116*, 10779.

[12] Khoroshun, D. V.; Inagaki, A.; Suzuki, H.; Vyboishchikov, S. F.; Musaev, D. G.; Morokuma, K. *J. Am. Chem. Soc.* **2003**, *125*, 9910.

[13] Riehl, J.-F.; Koga, N.; Morokuma, K. *Organometallics* **1994**, *13*, 4765.

[14] Inagaki, A.; Musaev, D. G.; Toshifumi, T.; Suzuki, H.; Morokuma, K. *Organometallics* **2003**, *22*, 1718.

10.1021/om060700y CCC: $37.00

Scheme 1. Associative Mechanism of the Hydride Exchange Proposed by Suzuki et al.[3]

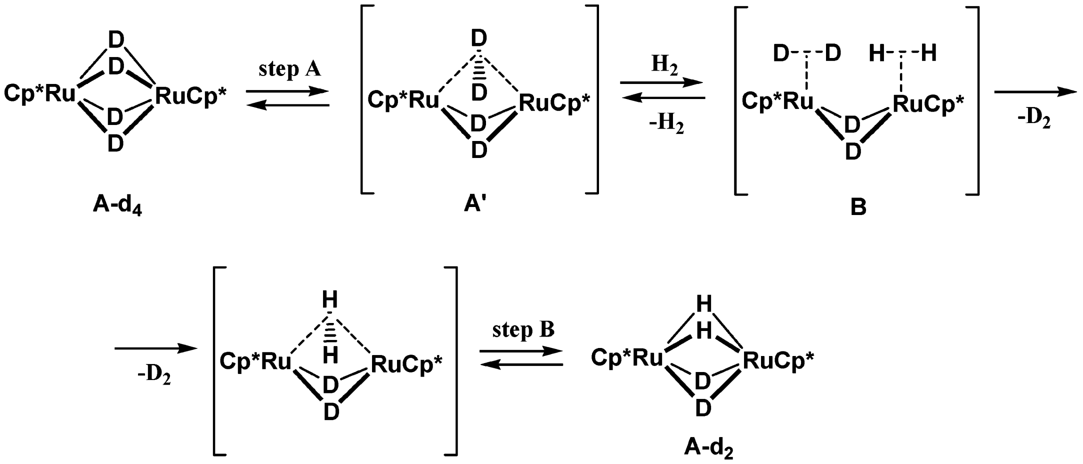

pressure at room temperature in toluene solution. The exchange reaction of deuteride ligands in Cp*Ru(μ-D)$_4$RuCp* (**A-d$_4$**) with hydrogen,

$$\mathrm{Cp^*Ru(\mu\text{-}D)_4RuCp^*} + 2\mathrm{H_2} \rightleftarrows \mathrm{Cp^*Ru(\mu\text{-}H)_4RuCp^*} + 2\mathrm{D_2}$$

was monitored by Suzuki et al. using NMR techniques.[3] In principle, the hydride exchange can occur via either an associative or dissociative pathway. Based on the temperature-dependent ^{1}H NMR studies, the associative mechanism shown in Scheme 1 was suggested. It includes the formation of the active intermediate dihydrogen complex **A′** and coordination of the incoming dihydrogen to form the hexahydride complex **B**, which was postulated to be actually a bis(dihydrogen) complex. The latter subsequently undergoes hydrogen exchange and eventually hydrogen elimination through the reverse process. The suggested mechanism was in two aspects influenced by an earlier work by Koga and Morokuma,[15] employing the simplified complex CpRu(μ-H)$_4$RuCp (**1**). First, the existence of **1′**,

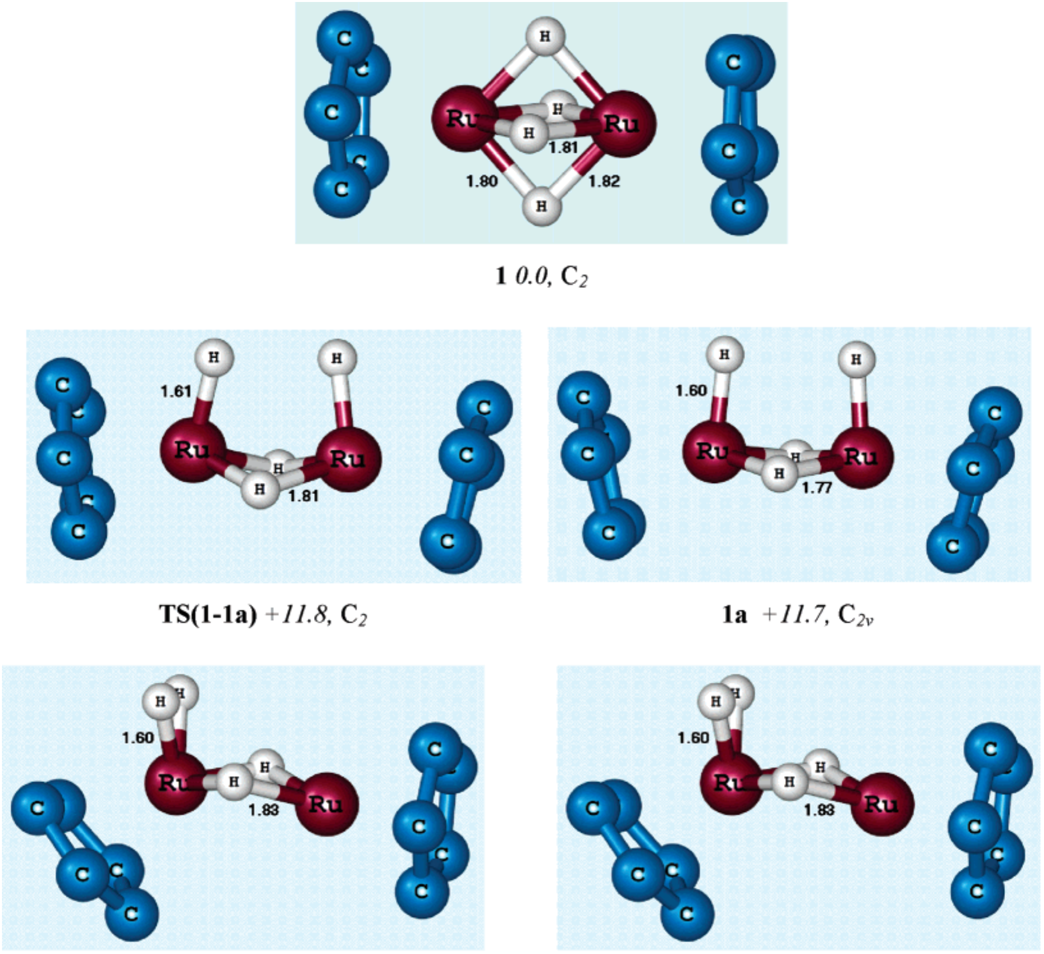

1 *0.0*, C$_2$

TS(1-1a) +*11.8*, C$_2$

1a +*11.7*, C$_{2v}$

1b +*13.7*

TS(1-1b) +*13.8*

Figure 1. Optimized structures of **1**, **1a**, and **1b** and the transition states **TS(1−1a)** and **TS(1−1b)**. The selected bond lengths are in Å. The relative Gibbs free energies are in kcal·mol^{-1}. Here and further the hydrogen atoms of the Cp rings are omitted for clarity.

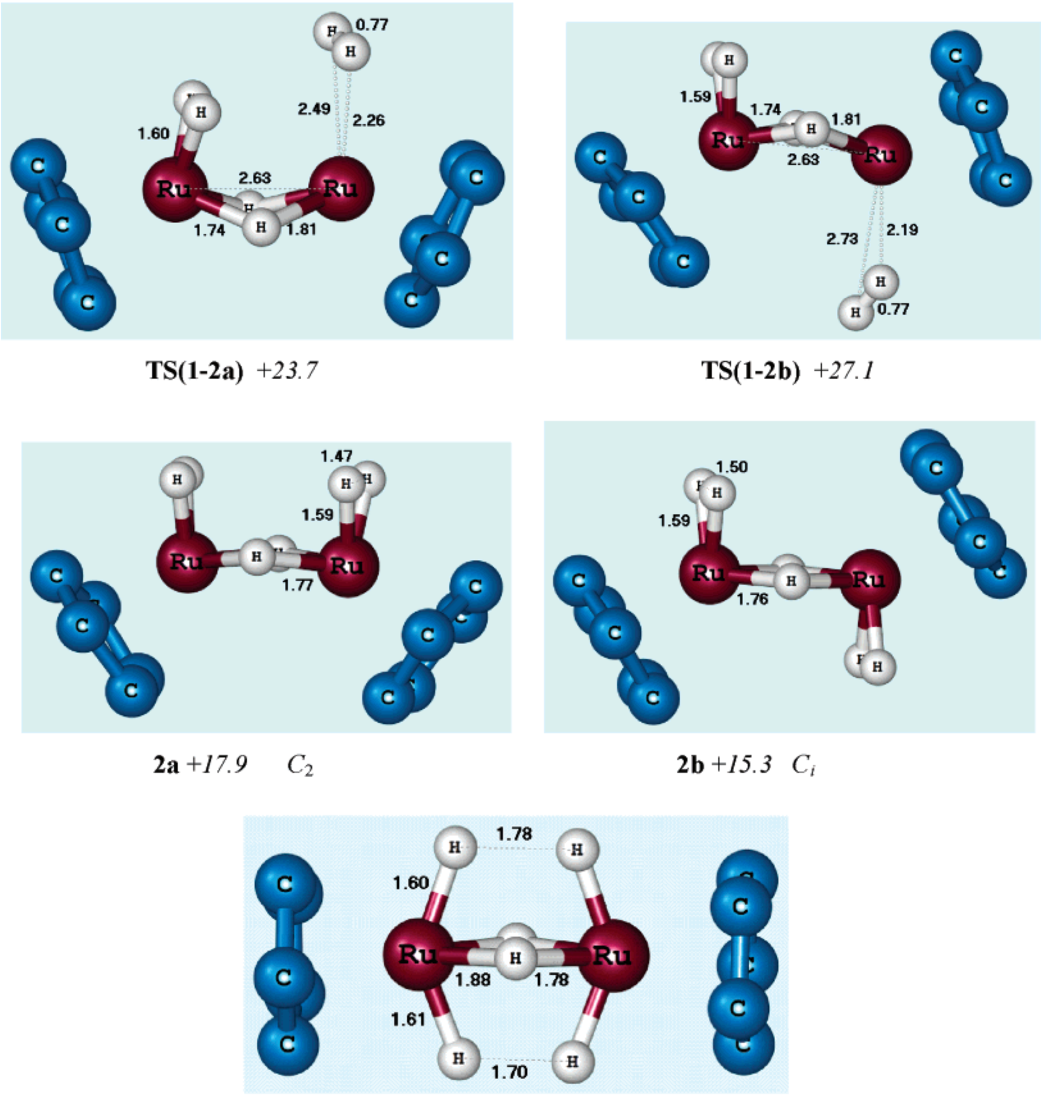

TS(1-2a) *+23.7* **TS(1-2b)** *+27.1*

2a *+17.9* C_2 **2b** *+15.3* C_i

2d *+36.1*

Figure 2. Optimized structures of the hexahydride complexes $Cp_2Ru_2(H)_6$ **2a**, **2b**, and **2d**, as well as the transition states **TS(1−2a)** and **TS(1−2b)** corresponding to their formation from **1** and dihydrogen. The selected bond lengths are in Å. The relative Gibbs free energies are in kcal·mol^{-1}.

analogous to **A′**, was predicted by Koga and Morokuma at the Hartree−Fock level using a rather small basis set. However, the single-point HF//MP2 calculations placed **1′** higher on the energy scale than the corresponding transition state between **1** and **1′**, thus making the existence of **1′** questionable.[15] Second, Koga and Morokuma's HF//MP2 calculations[15] indicated that the dihydrogen dissociation from **1** to give coordinatively unsaturated CpRu(μ-H)$_2$RuCp is very endothermic (+57 kcal·mol^{-1}). Thus, the dissociative exchange mechanism according to the scheme

$$\mathrm{CpRu}(\mu\text{-H})_4\mathrm{RuCp} \rightleftarrows \mathrm{CpRu}(\mu\text{-H})_2\mathrm{RuCp} + \mathrm{H}_2 \rightleftarrows \mathrm{CpRu}(\mu\text{-H})_4\mathrm{RuCp}$$

was rejected.

In this work, we present a computational study of the mechanism of the intermolecular exchange of hydrides in the complex CpRu(μ-H)$_4$RuCp with dihydrogen. Our primary purpose is to establish a detailed mechanism of the reaction, taking into account Suzuki's suggestion, by locating possible intermediates and the transition states. Both the associative and dissociative routes have been examined.

Computational Details

The computational study was performed with the simplified complex CpRu(μ-H)$_4$RuCp (**1**). The replacement of Cp* by the cyclopentadienyl ligand (Cp) should not critically affect the chemistry, but allows for large savings of computer time.

The quantum-chemical calculations were carried out using the density functional theory (DFT)[16] with the Gaussian 03 program package.[17] The gradient-corrected BP86 functional was employed, which combines Becke's nonlocal exchange[18] and Perdew correlation[19] functionals. We used the quasi-relativistic effective core potential of LaJohn et al. with the associate triple-ζ valence basis set[20] for ruthenium, 6-311G(d,p)[21] for the hydride hydrogens, and 6-31G(d,p)[22] for the spectator Cp ligands. For transition metal compounds, the chosen DFT approach (BP86 functional with

---

(15) Koga, N.; Morokuma, K. *J. Mol. Struct.* **1993**, *300*, 181.

(16) (a) Parr, R. G.; Yang, W. *Density Functional Theory of Atoms and Molecules*; Oxford University Press: New York, 1989. (b) Koch, W. Holthausen, M. C. *A Chemist's Guide to Density Functional Theory*; Wiley-VCH: Weinheim, 2000.

Table 1. Relative Electronic (ΔE_e) and Gibbs Free Energies (ΔG°_{298}) of Formation, and Entropy Contribution to Gibbs Free Energies ($-T\Delta S^{\circ}_{298}$) of the Reactant, Intermediates, and Products of Reaction 1[a]

molecule	ΔE_e, kcal·mol^{-1}	ΔG°_{298}, kcal·mol^{-1}	$-T\Delta S^{\circ}_{298}$, kcal·mol^{-1}
1 + H_2	0.0	0.0	0.0
1a + H_2	10.7	11.7	−0.9
TS(1−1a) + H_2	10.9	11.8	−0.5
1b + H_2	13.7	13.7	−1.3
TS(1−2a)	16.1 (12.5)	23.7 (21.1)	6.1
TS(1−2b)	17.7 (14.6)	27.1 (23.4)	7.6
2a	7.7 (5.6)	17.9 (13.5)	7.6
TS(2a−2a′)	7.8	16.1	7.0
2a′	6.2	16.7	7.3
2a″	5.9	16.2	7.2
2a‴	6.4	17.9	7.7
TS(2a‴−2c)	12.8	22.9	8.6
2b	5.8 (3.7)	15.3 (14.4)	7.0
TS(2b−2b′)	6.1	14.9	7.1
2b′	5.3	16.0	7.7
2b″	5.9	15.9	7.3
2b‴	5.7	15.6	6.7
2c	10.9	21.9	8.0
TS(2c−2c′)	11.6	21.3	8.1
2c′	11.6	21.4	7.3
2d	25.8	36.1	7.6
3 ($Ru_2H_2Cp_2$) + 2H_2	36.9	27.3	−9.1
TS(1−3) + H_2	36.3	34.2	−12.2

[a] Numbers in parentheses denote B3LYP results with the same basis set.

moderately large basis sets) normally provides realistic geometries, relative energies, and vibrational frequencies.[16b,23] Metal hydride complexes are no exception.[23e] A number of test calculations for the reactant CpRu(μ-H)$_4$RuCp show that the chosen level of theory is well suited to describe the system under study. In selected cases, we additionally performed calculations using B3LYP,[24] the hybrid functional combining Becke's exchange[18] with Hartree−Fock exchange along with the Lee−Yang−Parr[25] correlation functional. Hybrid functionals are normally considered superior to but more expensive than pure functionals.[16b,] The reactant, transition-state, and product geometries were fully optimized without any constraints. The nature of the optimized stationary points was confirmed by analytic computation of harmonic force constants. The transition states were connected to the related minima by means of an energy minimization following a small geometry displacement along the reaction coordinate obtained from the vibrational frequency calculation. For the sake of clarity, the frequency calculations were done using the ^{1}H isotope of hydrogen.

Results and Discussion

A. The Reactant and Its Isomers. In the course of the computations, a number of structures of general formula $Cp_2Ru_2(H)_4$ have been found. They are shown in Figure 1. Expectedly, the fourfold-bridged structure corresponding to the formula **1** (CpRu(μ-H)$_4$RuCp) was found to be the global minimum. It has C_2 symmetry, which is consistent with local symmetry of the molecule **A** found in the crystal structure.[3] The C_{2v} configuration is about 2 kcal·mol^{-1} less stable and has one imaginary frequency, corresponding to internal rotation of the Cp rings about the Ru−Ru axis. In the C_2 structure the H···H distances are almost equivalent (1.87−1.88 Å), showing no H−H bonds. The calculated Ru−Ru distance of 2.463 Å is very close to the experimental value.

According to the mechanism proposed by Suzuki and coworkers,[3] the first step in the hydrogen exchange reaction should be the formation of an active intermediate bis(hydride)−dihydrogen complex, **A′** (Scheme 1). When studying the dihydrogen dissociation from **1**, Koga and Morokuma[15] found that **1′** is 25 kcal·mol^{-1} higher in energy than **1** at the HF//MP2 level. However, a thorough scan of the potential energy surface (PES) performed by us at the BP86 level did not reveal any minimum of the **1′** type. The optimization of the starting geometry of **1′** with dihydrogen rotated 90° out-of-plane with the H−H bond collinear to the Ru−Ru vector leads to the structure **1a** (Figure 1). It contains two terminal hydrides placed at each metal center in *cis* orientation with respect to each other and is 11.7 kcal·mol^{-1} less stable than **1** in terms of ΔG°_{298}. An analogous *trans* complex does not exist, as the corresponding configuration easily collapses to **1**. However, another minimum with two terminal hydride ligands, labeled **1b**, has been found. In **1b**, both terminal hydrides are located on the same ruthenium atom, thus leaving the other ruthenium highly unsaturated. The Gibbs free energy ΔG°_{298} of **1b** is 13.8 kcal·mol^{-1} higher than that of **1**.

The free energy barriers $\Delta G^{\ddagger}_{298}$ for the conversion of **1a** or **1b** into **1** via the transition states **TS(1−1a)** and **TS(1−1b)**, respectively, are just 0.1 kcal·mol^{-1} each (Figure 1). Moreover, a slight geometry change in **1a** or **1b** results in a collapse of terminal hydrides to give **1**. This indicates that **1a** and **1b** are extremely shallow and narrow minima. Therefore, they do not play any significant role in the kinetics of the reaction.

B. The Associative Pathway. Now we are in a position to discuss the process of coordination of the H_2 molecule to **1**. To envisage possible resulting hexahydride structures, it is easier to start by formally attaching two hydrides to either the **1a** or **1b** structure. The subsequent opimizations result in the **2d** and **2a** (*cis*) and **2b** (*trans*) hexahydride complexes, respectively, containing two bridging and four terminal hydrides (Figure 2). The former structure, **2d**, is very high in energy (ΔG°_{298} =

---

(17) Frisch, M. J.; Trucks, G. W.; Schlegel, H. B.; Scuseria, G. E.; Robb, M. A.; Cheeseman, J. R.; Montgomery, J. A.; Vreven, T., Jr.; Kudin, K. N.; Burant, J. C.; Millam, J. M.; Iyengar, S. S.; Tomasi, J.; Barone, V.; Mennucci, B.; Cossi, M.; Scalmani, G.; Rega, N.; Petersson, G. A.; Nakatsuji, H.; Hada, M.; Ehara, M.; Toyota, K.; Fukuda, R.; Hasegawa, J.; Ishida, M.; Nakajima, T.; Honda, Y.; Kitao, O.; Nakai, H.; Klene, M.; Li, X.; Knox, J. E.; Hratchian, H. P.; Cross, J. B.; Bakken, V.; Adamo, C.; Jaramillo, J.; Gomperts, R.; Stratmann, R. E.; Yazyev, O.; Austin, A. J.; Cammi, R.; Pomelli, C.; Ochterski, J. W.; Ayala, P. Y.; Morokuma, K.; Voth, G. A.; Salvador, P.; Dannenberg, J. J.; Zakrzewski, V. G.; Dapprich, S.; Daniels, A. D.; Strain, M. C.; Farkas, O.; Malick, D. K.; Rabuck, A. D.; Raghavachari, K.; Foresman, J. B.; Ortiz, J. V.; Cui, Q.; Baboul, A. G.; Clifford, S.; Cioslowski, J.; Stefanov, B. B.; Liu, G.; Liashenko, A.; Piskorz, P.; Komaromi, I.; Martin, R. L.; Fox, D. J.; Keith, T.; Al-Laham, M. A.; Peng, C. Y.; Nanayakkara, A.; Challacombe, M.; Gill, P. M. W.; Johnson, B.; Chen, W.; Wong, M. W.; Gonzalez, C.; Pople, J. A. *Gaussian 03*, Revision C.02; Gaussian, Inc.: Wallingford, CT, 2004.

(18) Becke, A. D. *Phys. Rev. A* **1988**, *38*, 3098.

(19) Perdew, J. P. *Phys. Rev. B* **1986**, *33*, 8822.

(20) LaJohn, L. A.; Christiansen, P. A.; Ross, R. B.; Atashroo, T.; Ermler, W. C. *J. Chem. Phys.* **1987**, *87*, 2812.

(21) Krishnan, R.; Binkley, J. S.; Seeger, R.; Pople, J. A. *J. Chem. Phys.* **1980**, *72*, 650.

(22) Hehre, W. J.; Ditchfield, R.; Pople, J. A. *J. Chem. Phys.* **1972**, *56*, 2257.

(23) (a) Ziegler, T. *Chem. Rev.* **1991**, *91*, 651. (b) Ziegler, T. *Can. J. Chem.* **1995**, *73*, 743. (c) Jonas, V.; Thiel, W. *J. Chem. Phys.* **1995**, *102*, 8474. (d) See special issue on computational Transition Metal Chemistry: *Chem. Rev.* **2000**, *100*, 351−818. (e) Maseras, F.; Lledós, A.; Clot, E.; Eisenstein, O. *Chem. Rev.* **2000**, *100*, 601.

(24) (a) Becke, A. D. *J. Chem. Phys.* **1993**, *98*, 5648. (b) Stephens, P. J.; Devlin, F. J.; Frisch, M. J.; Chabalowski, C. F. *J. Phys. Chem.* **1994**, *98*, 11623.

(25) (a) Lee, C.; Yang, W.; Parr, R. G. *Phys. Rev. B* **1988**, *37*, 785. (b) Miehlich, B.; Savin, A.; Stoll, H.; Preuss, H. *Chem. Phys. Lett.* **1989**, *157*, 200.

(26) Görling, A.; Trickey, S. B.; Gisdakis, P.; Rösch, N. *Top. Organomet. Chem.* **1999**, *4*, 109.

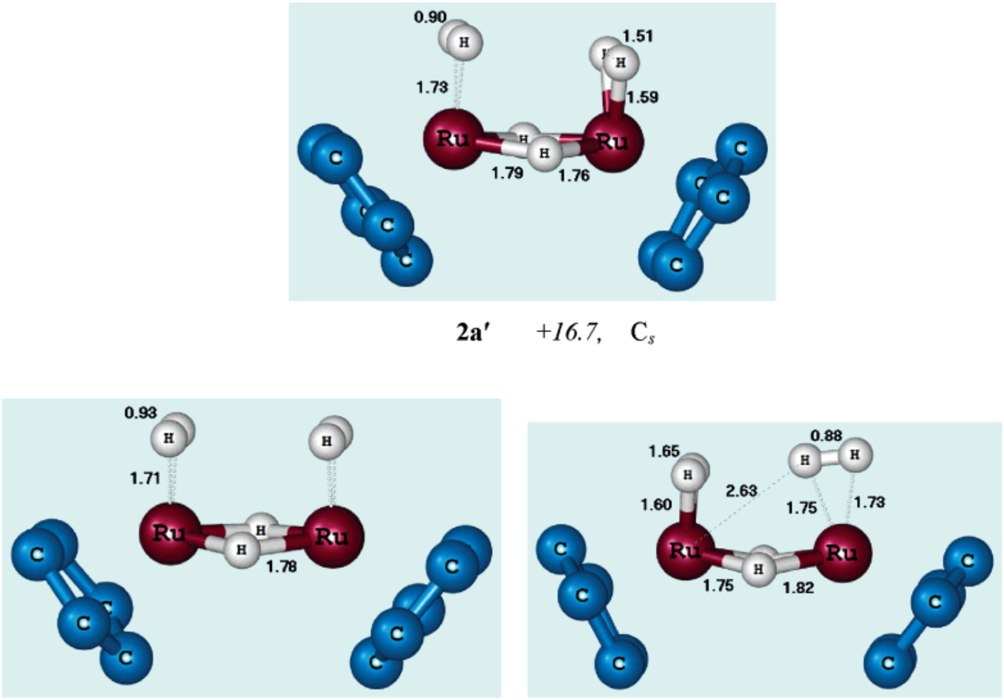

2a′ *+16.7*, C$_s$

2a″ *+16.2*, C$_2$ **2a‴** *+17.9*, C$_s$

Figure 3. Optimized structures of *cis* dihydrogen−hydride complexes $Cp_2Ru_2(H)_6$ with selected bond lengths (in Å) and the relative Gibbs free energies (in kcal·mol^{-1}).

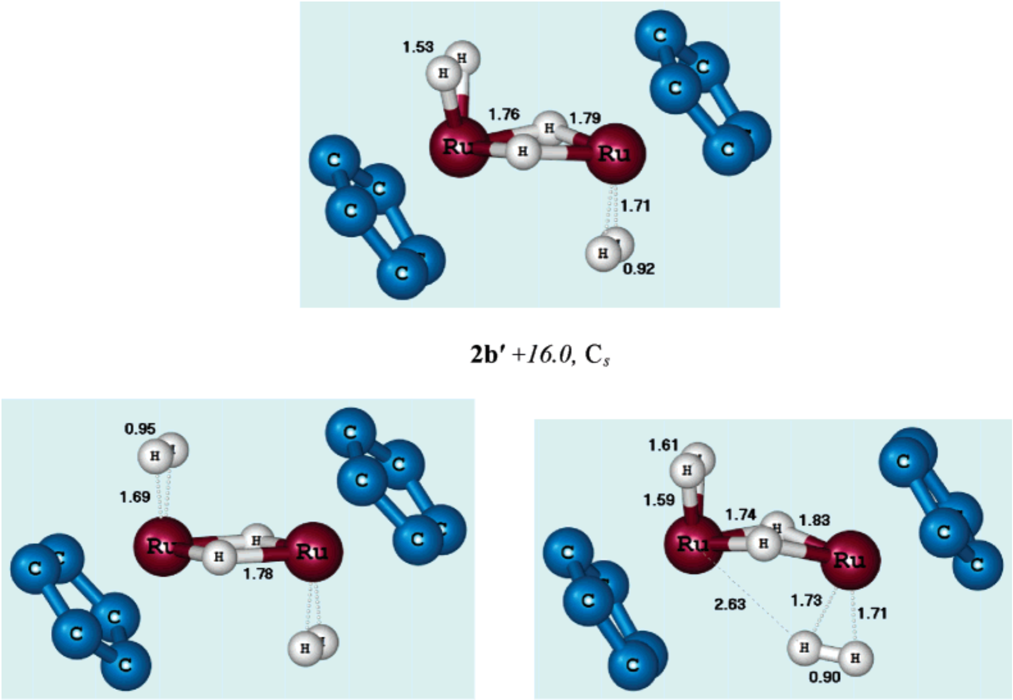

2b′ *+16.0*, C$_s$

2b″ *+15.9*, C$_{2h}$ **2b‴** *+15.6*, C$_s$

Figure 4. Optimized structures of *trans* dihydrogen−hydride complexes $Cp_2Ru_2(H)_6$ with selected bond lengths (in Å) and the relative Gibbs free energies (in kcal·mol^{-1}).

+36.1 kcal·mol^{-1}) and is unlikely to play any role in the mechanism of the hydrogen exchange reaction. Compared to it, **2a** and **2b** are substantially more stable, although their formation is also endothermic (ΔE_e = 7.7 and 5.8 kcal·mol^{-1}, respectively (Table 1); ΔG°_{298} = 17.9 and 15.3 kcal·mol^{-1}, respectively). In fact, the structures **2a** and **2b** are formed directly from **1** through the transition states **TS(1−2a)** and **TS-(1−2b)**, correspondingly, with substantial barriers ($\Delta G^\ddagger_{298}$ = 23.7 and 27.1 kcal·mol^{-1}, respectively; $\Delta E^\ddagger_e$ =16.1 and 17.7 kcal·mol^{-1}, respectively). These barriers reflect high structure reorganization costs. As seen in Figure 2, the formation of the

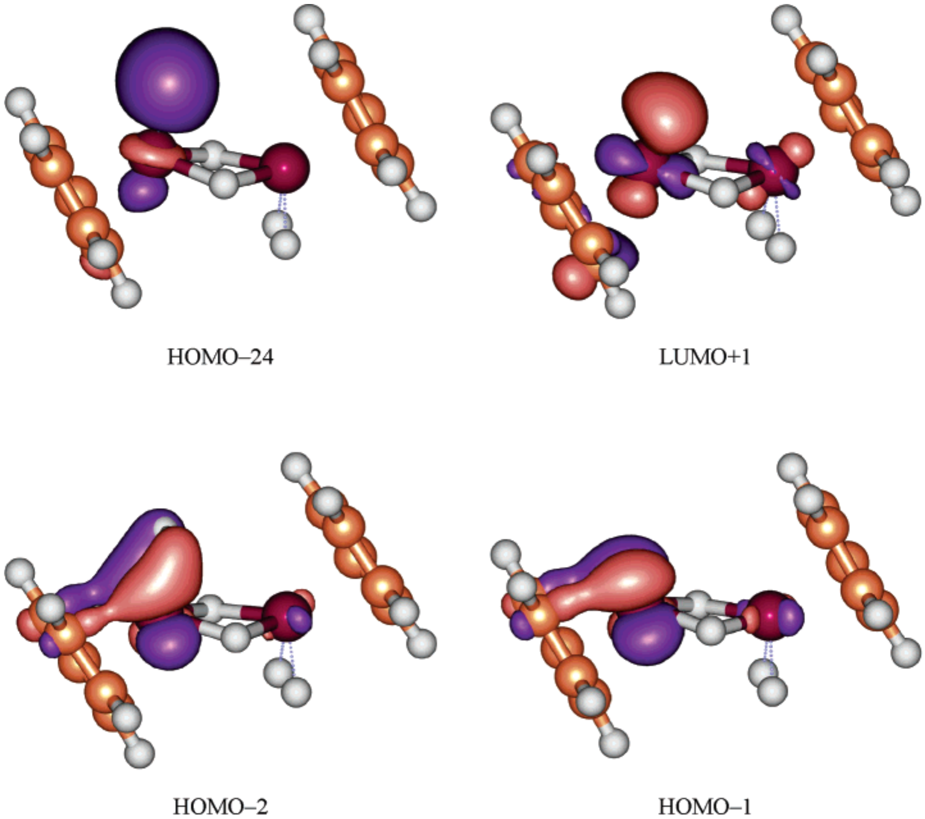
HOMO–24
LUMO+1
HOMO–2
HOMO–1

Figure 5. Orbitals of the hexahydride complex **2b′** (left) relevant to the Ru−H_2 bonding and their counterparts in the CpRu(μ-H)$_2$Ru(H)$_2$Cp fragment (right).

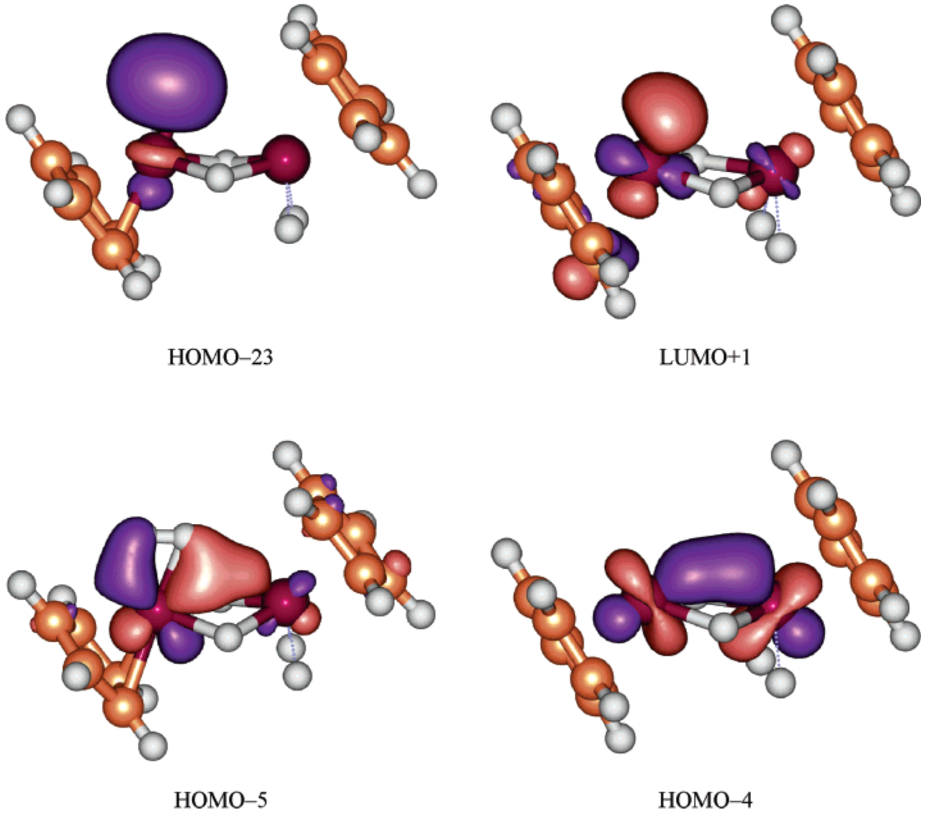
HOMO–23
LUMO+1
HOMO–5
HOMO–4

Figure 6. Orbitals of the hexahydride complex **2b‴** (left) relevant to the Ru−H_2 bonding and their counterparts in the CpRu(μ-H)$_2$Ru(H)$_2$Cp fragment (right).

hexahydride complexes can be conceived as a rearrangement of the coordination sphere in **1** to generate a vacant site on one of the ruthenium atoms followed by the binding of the incoming H_2 molecule to the now unsaturated ruthenium. The higher energy of **TS(1−2b)** compared to **TS(1−2a)** can be understood from the consideration of their geometries. The formation of the former requires a larger displacement of the (H)$_4$ moiety under impact of the incoming hydrogen molecule. The Ru⋯H

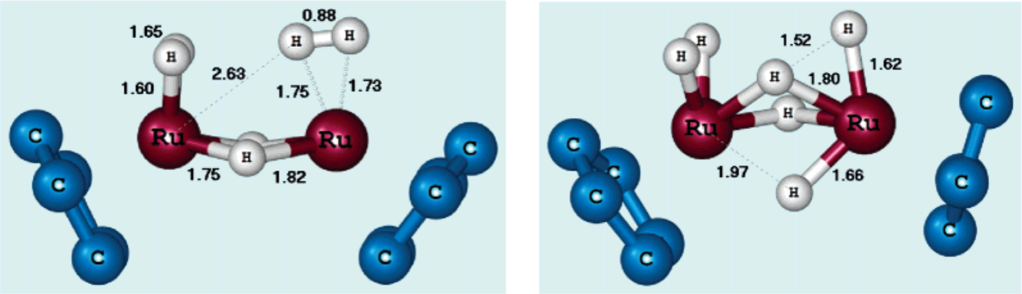

2a‴ *+17.9*, C_s **TS(2a‴-2c)** *+22.9*

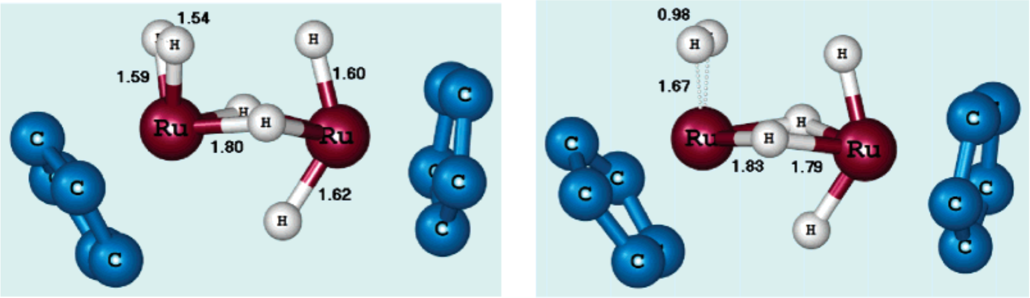

2c +21.*9*, C_s **2c′** +21.*4*, C_s

Figure 7. Optimized structures of the hexahydride complexes **2a‴**, **2c**, and **2c′** and the transition state connecting **2a‴** and **2c** with selected bond lengths (in Å). The relative Gibbs free energies are in kcal·mol^{-1}.

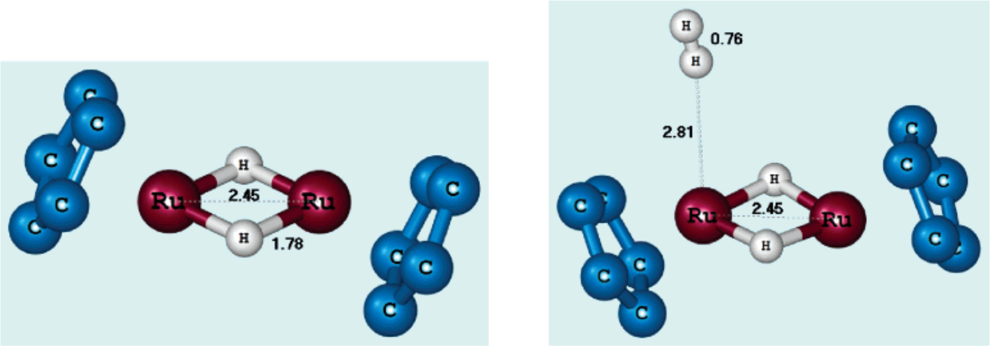

3 *+27.3* **TS(1-3)**, *+33.2*

Figure 8. Optimized structures of the dihydride complexes **3** (CpRu(μ-H)$_2$RuCp) and the transition state **TS(1−3)** connecting **1** with **3**. Selected bond lengths are in Å. The relative Gibbs free energies are in kcal·mol^{-1}.

distances in the transition states differ by 0.2 Å in **TS(1−2a)** and more strongly—by 0.5 Å—in **TS(1−2b)**. However, in both transition states the H−H bond of the incoming H_2 is elongated only by about 0.02 Å compared to the free hydrogen molecule.

For the sake of comparison, we performed test calculations of the complexes **2a**,**b** using the B3LYP functional. The formation barriers are about 3 kcal·mol^{-1} lower than at BP86 ($\Delta G^{\ddagger}_{298}$ = 21.1 and 23.4 kcal·mol^{-1}; $\Delta E^{\ddagger}_{e}$ = 12.5 and 14.6 kcal·mol^{-1} for **2a** and **2b** at B3LYP, respectively). As the B3LYP functional is generally considered to be more reliable, the barriers in reality are expected to be somewhat lower than the BP86 values.

The Ru−H$^{\text{bridge}}$ bonds in **2a** and **2b** are about 0.05 Å shorter than in **1**, while the Ru−Ru distance in **2a** and **2b** is 0.06 Å longer than in **1**. The Ru atoms and the two bridging hydrides in **2a** and **2b** are nearly in the same plane. In both **2a** and **2b** the distance between geminal hydrides is about 1.5 Å, which allows one to characterize them as classical hydride complexes. We found that along with the classical hydride complexes **2a** and **2b** there exist the corresponding dihydrogen complexes **2a′**−**2a‴** (Figure 3) and **2b′**−**2b‴** (Figure 4). The conversion of **2a** and **2b** to the corresponding dihydrogen complexes **2a′**, **2a″** and **2b′**, **2b″**, respectively, proceeds through the simultaneous elongation of Ru−H bond and the shortening of the H−H distance. In addition, two more dihydrogen complexes, **2a‴** and **2b‴**, were located by internal rotation of dihydrogen by 90° in **2a′** and **2b′**, respectively. The H_2 ligand in **2a‴** and **2b‴** is collinear to the Ru−Ru vector. The Ru−H and H−H bond lengths in **2a‴** and **2b‴** are close to each other and to those in **2a″** and **2b″**.

One of the Ru atoms in **2a′** and **2b′** has coordination close to trigonal-pyramidal, while the other has a tetragonal-pyramidal environment. The H−H bond in the bis(dihydrogen) complexes **2a″** and **2b″** is elongated by 0.17 and 0.19 Å, respectively, indicating a strong back-donation from ruthenium to η^2-H_2. Slightly less lengthening of H−H bond is observed in the dihydrogen complexes **2a′** and **2b′** (0.14 and 0.17 Å, respectively) and in **2a‴** and **2b‴** (0.12 and 0.14 Å).

Scheme 2. Calculated Steps of the Hydrogen Exchange Reaction[a]

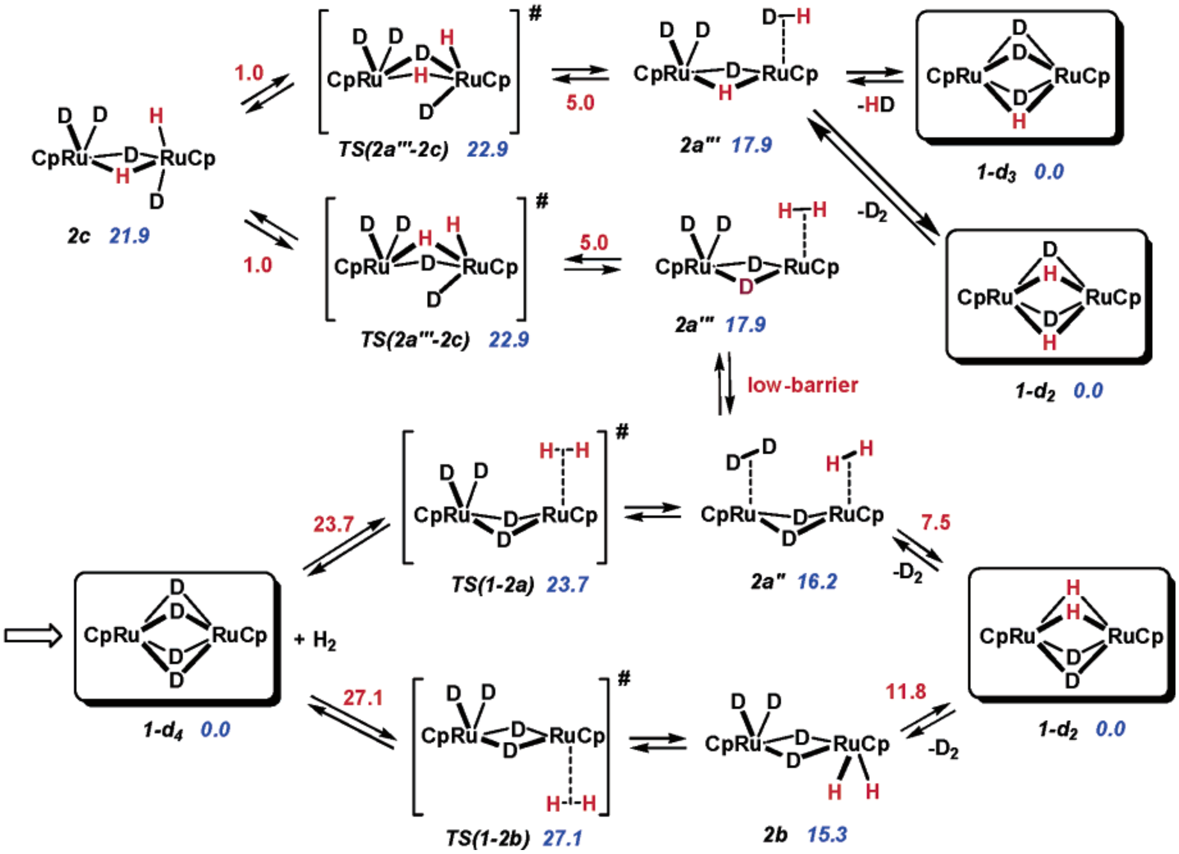

[a] Relative Gibbs free energies are in kcal·mol^{-1}. The ΔG°_{298} values were calculated using the ^{1}H isotope of hydrogen.

It is interesting to consider different ways of coordination of dihydrogen from the orbital viewpoint. For this purpose, the orbitals of **2b′** and **2b‴** relevant for $H_2 \rightarrow$ Ru σ-donation and Ru $\rightarrow H_2$ π-back-donation are depicted in Figures 5 and 6, respectively. The virtual LUMO+1 orbital of the CpRu(μ-H)$_2$Ru(H)$_2$Cp fragment is suitable for the $H_2 \rightarrow$ Ru donation for both the perpendicular (as in **2b′**, Figure 5) and collinear (as in **2b‴**, Figure 6) orientation of the H_2 ligand. As a result, a rather low-lying molecular orbital (HOMO−24 in the case of **2b′**, HOMO−23 in the case of **2b‴**) emerges. For the back-donation to the σ*-orbital of H_2, the suitable orbitals of the CpRu(μ-H)$_2$Ru(H)$_2$Cp fragment are HOMO−2 for the perpendicular coordination in **2b′** (Figure 5) and HOMO−4 for the collinear coordination in **2b‴** (Figure 6). As HOMO−4 lies 0.05 hartree lower than HOMO−2, the back-donation for the collinear H_2 orientation should be lower than for the perpendicular case. This partly explains why the orientation of H_2 collinear to the Ru−Ru vector is energetically less favorable.

The most stable isomer of *cis*-$Cp_2Ru_2H_6$ is the bis(dihydrogen) complex **2a‴**, whereas in the case of *trans*-$Cp_2Ru_2H_6$ it is the classical hydride complex **2b**. The difference in free energy between the most and the least stable isomer of *cis*- and *trans*-hexahydride is only 2.0 and 0.7 kcal·mol^{-1}, respectively. The scan of the PES reveals that the dihydrogen−hydride conversion proceeds with a negligible barrier; that is, two hydrogen atoms move almost freely in a large region within the coordination sphere of the metal. Such fluxionality between hydride and dihydrogen complexes is a rather common phenomenon for late transition metal complexes.

In the course of a PES scan, the isomer **2c** has been found (Figure 7). **2c** is a classical hexahydride complex and is lower in energy than **2a″** and **2b** by 6−7 kcal·mol^{-1}. Effectively, the formation of **2a‴** from **2c** occurs through substitution of one of the bridging hydrides by one of the hydrogen atoms of the dihydrogen ligand in **2a‴** such that the former becomes terminal at the opposite side of the Ru−H−Ru−H ring. This interesting process demonstrates the mobility of hydride ligands in this system and can be understood from the structure of the corresponding transition state **TS(2a‴−2c)** (Figure 7). The transition state **TS(2a‴−2c)** is a late one. The H···H distance in it is 1.52 Å. The barrier for the **2a″** → **2a‴** → **2c** isomerization is non-negligible ($\Delta G^{\ddagger}_{298}$ = 6.7 kcal·mol^{-1}). Since it is comparable to the barrier of the dihydrogen dissociation from **2a″** via **2a** and **TS(1−2a)** ($\Delta G^{\ddagger}_{298}$ = 7.5 kcal·mol^{-1}), the two processes will compete. The barrier for the reverse step **2c** → **2a‴** is very low ($\Delta G^{\ddagger}_{298}$ = 1.0 kcal·mol^{-1}), which indicates that **2c** is a shallow minimum and the reverse step is very fast.

C. The Dissociative Pathway. The dissociative pathway is by far easier to perceive, since it consists basically in the dissociation of the reactant **1** to form the unsaturated complex CpRu(μ-H)$_2$RuCp. Only the *trans* structure of CpRu(μ-H)$_2$RuCp (**3**) was found to be a minimum (Figure 8). The Gibbs free energy ΔG°_{298} for the dissociation of **1** to give **3** is 27.3 kcal·mol^{-1}, while ΔE_e is about 37 kcal·mol^{-1}. The dissociation occurs asymmetrically, with two of the bridging hydrides of **1** moving toward one of the ruthenium atoms and finally eliminating dihydrogen. As this process is associated with both Ru−H bond breaking and H−H bond formation, it should go through a transition state. As expected for a highly endothermic process, this transition state **TS(1−3)** is a late one, with the H−H bond already formed and a very long Ru···H_2 separation. The $\Delta G^{\ddagger}_{298}$ barrier is 34.2 kcal·mol^{-1}. Although the ΔG°_{298} and $\Delta G^{\ddagger}_{298}$ for the hydrogen dissociation are not as unfavorable as the dissociation energy reported previously,[15] they are by far less favorable than the corresponding values for the associative mechanism. Therefore, the dissociative mechanism should be discarded, in agreement with Suzuki's suggestion.[3]

Conclusions

We have considered both dissociative and associative mechanisms for the hydrogen exchange in **1** (CpRu(μ-H)$_4$RuCp). The former proceeds through the dissociation of dihydrogen to afford CpRu(μ-H)$_2$RuCp. The barrier for this process, with $\Delta G^{\ddagger}_{298}$ about 34 kcal·mol^{-1}, is prohibitively high.

Much more affordable is the associative mechanism, which occurs through hexahydride intermediates Cp$_2$Ru$_2$(H)$_6$. The reaction steps of the associative mechanism with their respective intermediates and transition states are summarized in Scheme 2. There are in turn two possible pathways, going through either the *cis* complex **2a″** or *trans* complex **2b**. The $\Delta G^{\ddagger}_{298}$ barriers are 23.7 and 27.1 kcal·mol^{-1}, respectively. This turns out to be the rate-determining step. Therefore, the *cis* pathway is preferred. The subsequent hydrogen elimination from **2a″** to yield **1** (denoted as **1-d$_2$** in Scheme 2) has a $\Delta G^{\ddagger}_{298}$ barrier of 7.5 kcal·mol^{-1}. Alternatively, the intermediate **2a″** can transform via **2a‴** and **TS(2a‴−2c)** to **2c** with the total $\Delta G^{\ddagger}_{298}$ barrier of 6.7 kcal·mol^{-1}. Thus, the direct dihydrogen elimination competes with the isomerization processes involving interchanging of bridging and terminal hydrides.

In the reverse step, which is a low-barrier process, the terminal hydride in **2c** can be exchanged by a bridging hydride. The intermediate **2a‴** can also undergo dihydrogen elimination to eventually afford **1**.

Note that the initial hydrogen coordination to give **2a″** or **2b** is strongly affected by entropy effects. As seen from the rightmost column of Table 1, the entropy contributes about 6−8 kcal·mol^{-1} to the $\Delta G°_{298}$ (and $\Delta G^{\ddagger}_{298}$) of this process in the gas phase. However, in solution the entropy effect is typically halved. On the other hand, the barrier calculated at B3LYP level, which is presumably superior, is about 3 kcal·mol^{-1} lower than the BP86 value. Thus, the actual barrier for the rate-determining step is expected to be below 20 kcal·mol^{-1}.

By and large, our calculations support Suzuki's conclusion[3] that the associative mechanism for the hydrogen exchange is more favorable than the dissociative one. On the other hand, our study demonstrates that the actual mechanism is by far more complicated than a simple hydrogen coordination and elimination, with many intermediates found. These intermediates can interchange bridging and terminal hydrides, thus contributing to the hydrogen exchange.

Acknowledgment. We thank Prof. Keiji Morokuma and Prof. Hiroharu Suzuki for attracting our attention to this field. Financial support from the Spanish Ministry of Education and Science (Ramón y Cajal Program and grant CTQ2005-02698) is highly appreciated. S.T. thanks the Generalitat de Catalunya for a graduate fellowship.

Supporting Information Available: (A) Geometry of the reactant 1 calculated using various functionals and basis sets; (B) list of Cartesian coordinates of the structures **1**, **1a**, **TS(1−1a)**, **1b**, **TS(1−2a)**, **TS(1−2b)**, **2a**, **TS(2a−2a′)**, **2a′**, **2a″**, **2a‴**, **TS(2a‴−2c)**, **2b**, **TS(2b−2b′)**, **2b′, 2b″, 2b‴**, **2c**, **TS(2c−2c′)**, **2c′**, **2d**, **3**, **TS(1−3)**. This material is available free of charge via the Internet at http://pubs.acs.org.

OM060700Y